Excitons, polarons, and laser action in poly(*p*-phenylene vinylene) films

R. Österbacka[a)]
Department of Physics, University of Utah, Salt Lake City, Utah 84112-0830
and Department of Physics, Åbo Akademi University, Porthansgatan 3, FIN-20500 Turku, Finland

M. Wohlgenannt
Department of Physics, University of Utah, Salt Lake City, Utah 84112-0830
and Department of Physics and Astronomy, The University of Iowa, Iowa City, Iowa 52242

M. Shkunov
Department of Physics, University of Utah, Salt Lake City, Utah 84112-0830
and Merck Specialty Chemicals Ltd., University Parkway, Chilworth, Southampton, Hants SO16 7QD, United Kingdom

D. Chinn
Department of Physics, University of Utah, Salt Lake City, Utah 84112-0830
and Sandia National Laboratories, MS 9671, Livermore, California 94551-0969

Z. V. Vardeny
Department of Physics, University of Utah, Salt Lake City, Utah 84112-0830

(Received 29 October 2002; accepted 20 February 2003)

We have used a multitude of linear and nonlinear cw optical spectroscopies to study the optical properties of water precursor poly(*p*-phenylene vinylene) (PPV) thin films. These spectroscopies include absorption, photoluminescence, photoinduced absorption and their respective optically detected magnetic resonance, and electroabsorption spectroscopy. We have studied singlet and triplet excitons, polarons, and laser action in PPV films. We found that the lowest-lying absorption band is excitonic in origin. It consists of two absorption components due to a bimodal distribution of the polymer chain conjugation lengths. Electroabsorption spectroscopy unambiguously shows the positions of the lowest-lying odd parity exciton $1B_u$ at 2.59 eV and two of the higher-lying even-parity excitons, namely, mA_g at 3.4 eV and kA_g at 3.7 eV. From these exciton energies we obtained a lower bound for the exciton binding energy in PPV, $E_b(\min)=E(mA_g)-E(1B_u)=0.8$ eV. The quantum efficiency spectrum for triplet exciton photogeneration consists of two contributions; the intersystem crossing and, at higher energies, singlet fission. From the onset of the singlet fission process at $E_{SF}=2E_T$, we could estimate the energy of the lowest-lying triplet exciton, $1\,^3B_u$, at 1.55 eV, with a singlet–triplet splitting as large as 0.9 eV. From photoinduced absorption spectroscopy we measured the triplet–triplet transition, $T\rightarrow T^*$, to be 1.45 eV. The quantum efficiency spectrum for polaron photogeneration also consists of two contributions: one extrinsic and the other intrinsic. The latter shows a monotonically increasing function of energy with an energy onset at 3.3 eV. The intrinsic photogeneration process is analyzed with a model of free-electron–hole pair photogeneration, which separate more effectively at higher energy. The carrier generation quantum yield at 3.65 eV is estimated to be 0.5%. The quantum efficiency for photoluminescence, on the other hand, shows one single step-function process, with an onset at 2.4 eV. The photoluminescence spectrum is well structured, showing five phonon side bands with 190 meV separation. We have also studied laser action in PPV thin films and microcavities such as microrings and microdisks. The effective gain spectrum is calculated and the estimated threshold excitation intensity for laser action for the 0-1 transition is found to be in good agreement with the data, with an estimated exciton density of 2×10^{18} cm^{-3}. Lasing from microring devices shows several narrow waveguide modes, with intermode spacing of 0.45 nm that corresponds to an effective mode refractive index, $n_{\text{eff}}=1.45$. The spectral width of the laser modes is resolution limited and gives a lower estimate of the cavity quality factor, Q. For microrings we found $Q>5000$, which is limited by self-absorption in the polymer film. © *2003 American Institute of Physics.* [DOI: 10.1063/1.1566937]

[a)]Electronic mail: rosterba@abo.fi

I. INTRODUCTION

Since the first report of electroluminescence (EL) in the organic polymer semiconductor poly(para-phenylene vinylene) (PPV),[1] an understanding of its low-lying excited electronic states has attracted considerable interest.[2–17] Yet, the magnitude of the electron–electron ($e-e$) interaction[18] and its role in determining the excited state energies and the photo-excitation properties in PPV is still unsettled.[6,7,10–16,19–21] Even the linear optical absorption has turned out to be controversial,[7,13–17,22–24] since the absorption bands are usually broadened by solid state effects, disorder, chemical impurities etc. One way to overcome this problem is to orient the polymer chains through stretching and measure polarized linear and nonlinear optical properties to determine the polarization of the various absorption bands.[25–27]

Since PPV is centrosymmetric (Fig. 1, upper inset) and thus possesses a C_{2h} point group symmetry, its electronic states are divided into odd- (B_u) and even- (A_g) parity symmetry. Among them the four essential singlet states,[20,21] which determine the photoluminescence (PL) efficiency and various optical nonlinear spectra are: the ground state, $1A_g$; the first excited B_u state, $1B_u$; an important A_g state, mA_g with strong coupling to the $1B_u$; and the continuum-band threshold, nB_u. Nonlinear spectroscopies such as two-photon absorption[3,28,29] and electroabsorption[30,31] have turned out to be very useful in obtaining information about the lowest-lying even- and odd-parity excitons.[30,32,33]

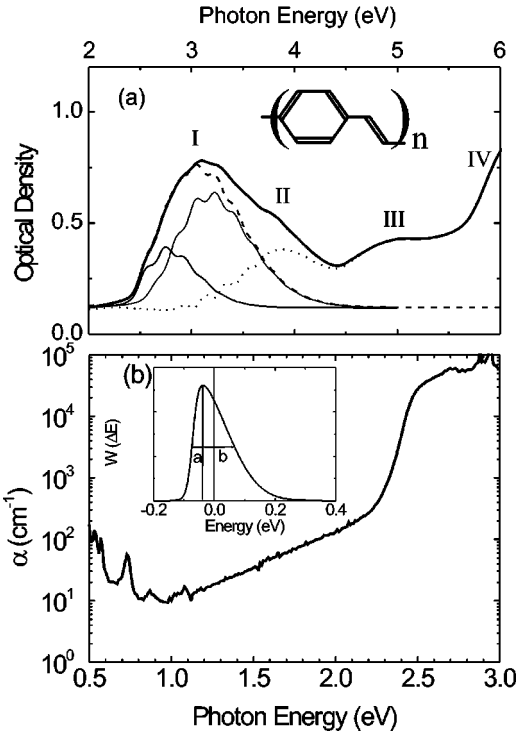

FIG. 1. (a) Measured (bold line) absorption spectrum of a PPV film compared to the absorption spectrum (dashed line) calculated from the bimodal conjugation-length distribution (thin solid lines). The four absorption bands are indicated in the figure while the difference spectrum (dotted line) between the measured and calculated $\alpha(\omega)$ shows evidence of a second absorption band at 3.9 eV. The upper inset shows the chemical structure of PPV. (b) PPV absorption spectrum measured by photothermal deflection in a thick film. The conjugation length distribution function $W(\Delta E)$ used in the calculation is shown in the lower inset. The width ($\gamma=a+b$) and asymmetry ($\delta=b/a$) can be calculated from the $W(\Delta E)$.

The observation of PL and EL and their high efficiency[34] implies that there is an allowed one-photon transition from the lowest singlet excitonic state $1B_u$ into the ground state, where the exciton binding energy is substantially large compared to kT.[35] Yan *et al.* suggested that the primary photoexcitations in PPV-type π-conjugated polymers are spatially indirect excitons, or polaron pairs,[36–38] but the idea has been challenged by several groups.[39–41] Since the lowest-lying excitons are relatively tightly bound, then the spin configuration of the spin-1/2 electron and spin-1/2 hole influences the binding energy, with the spin–triplet exciton lower in energy than the spin-singlet exciton by the exchange energy.[11] The energy separation, Δ_{ST}, between the lowest-lying singlet and triplet excitons may therefore provide an experimental method for measuring the magnitude of the $e-e$ interaction in PPV.

In this work we have studied the optical properties of unsubstituted PPV thin films, using several optical techniques related to long-lived charged and neutral photoexcitations, as well as laser action. We have used both linear and nonlinear optical spectroscopies, such as visible and infrared absorption spectroscopy, photothermal deflection spectroscopy (PDS), photoluminescence (PL), electroabsorption (EA), photo induced absorption (PA), PA detected magnetic resonance (PADMR), as well as their action spectra.

The paper is divided as follows: in Sec. II we outline the experimental techniques used in this study; in Secs. III A and III B, respectively we discuss the linear absorption and EA in PPV films; in Sec. III C (III D) we study the PA (PADMR) spectrum. The action spectra of longlived photo generated triplet excitons and polarons are studied in Secs. III E and III F, respectively. Laser action studies in PPV films and microcavities are described in Sec. III G.

II. EXPERIMENT

In this section we describe the cw-optical techniques used in our studies. For the photomodulation (PM) spectroscopy we used a standard PM setup with a modulated Ar^+ laser beam or a monochromatized xenon lamp as excitation (pump) and several incandescent light sources as probe beams that cover the spectral range $\hbar\omega$ from 0.1 to 3 eV. Photoinduced changes ΔT in the sample transmission, T were recorded with a phase sensitive technique to obtain the normalized changes in transmission, $\Delta T/T$. We define, PA as $\Delta\alpha=-\Delta T/Td=N\sigma d$, where d is the film thickness, N is the photoexcitation density, σ is their optical absorption cross section, and $\Delta\alpha$ is the change in absorption, α.

For PA (PL)-detected magnetic resonance [PADMR(PLDMR)] the sample was mounted in a high-Q microwave cavity at 3 GHz equipped with a superconducting magnet and illuminated by the pump and probe beams. Microwave resonant absorption leads to small changes, $\delta T(\delta\mathrm{PL})$, in the probe transmission (PL intensity). This $\delta T(\delta\mathrm{PL})$ is proportional to δN, which is induced by transitions in the microwave frequency range that change the spin-dependent recombination rates. Two types of PADMR spec-

tra are possible: the *H*-PADMR spectrum, in which δT is measured at a fixed probe wavelength, λ as the magnetic field H is varied. The other type is the λ-PADMR spectrum, in which δT is measured at a constant H in resonance, whereas λ is varied.

The action spectra of PL and PA were measured using an excitation beam from a 250 W Xe lamp passing through a monochromator, equipped with proper filters and gratings spanning a spectral range E from 1.5 to 4.5 eV. The pump beam fluence I was kept in the linear regime of the PA excitation intensity range to ensure that the lifetime of the excited species is independent of the light intensity.[42] We measured the quantum yield (QY) per absorbed photon, where ΔT (or PL) was multiplied by the factor $g(E)=(1/Ed)(1-R)I(E)(1-\exp(\alpha(E)d))$ where α and R are the film absorption and reflectivity spectrum, respectively and $I(E)$ is the pump intensity spectrum.

For the laser action studies we used for excitation the third harmonic of a Nd-doped yttrium aluminum garnet regenerative laser amplifier at 355 nm, with 100 ps pulse duration at a repetition rate of 100 Hz. The circular illuminated area on the sample was about 1 mm^2. The emission was collected by a short focusing lens and analyzed by a SPEX 0.6 m triple spectrometer with a liquid-nitrogen-cooled charge-coupled device camera. For the microlasers, the PPV was directly polymerized on a commercially available optical fiber of 125 μm in diameter. The excitation light was then focused in a plane perpendicular to the fiber axis so that only the microring was excited. The microdisks were fabricated with photolithography techniques,[43] and disks with diameters in the range of 80–200 μm were studied.

The PPV polymer was synthesized by the commonly used precursor route.[44] Here the water-soluble nonconjugated soluble polymer is cast into films and then converted to the desired polymer by heating it in flowing nitrogen at 220 °C, for at least 2 h.

III. RESULTS AND DISCUSSIONS

A. Absorption and photoluminescence spectroscopies

The absorption spectrum of our PPV films [Fig. 1(a)] shows an onset at about 2.5 eV and consists of several bands that were labeled before as I–V.[13,14,22,27] Absorption band I at $\simeq$3 eV is due to the main delocalized (d) $\pi-\pi^*$ transition; it is most probably the result of an inhomogeneously broadened $1A_g-1B_u$ excitonic transition. Band I shows a fairly well resolved vibronic structure on the low-energy side with a phonon energy of 190 meV. However, the high degree of asymmetry broadens the band on the high-energy side, giving a full width at half maximum (FWHM) of 1.2 eV. This asymmetry has been related to different chain packing in the nanocrystalline structure formed when using the precursor route.[33]

The strong absorption tail seen below the onset of the first absorption band [Fig. 1(a)] may be attributed to Rayleigh scattering of light from the microcrystallite structures formed in the film. In order to study the true absorption in this region we therefore used the technique of PDS as shown in Fig. 1(b); this technique is suitable for measuring small absorption coefficients below 10^4 cm^{-1}, since is not sensitive to scattering. Figure 1(b) shows a remarkably long absorption tail extending down to below 1 eV, which is probably due to the existence of impurities and defects in the film. The absorption coefficient drops exponentially over two orders of magnitude between 2.45 eV and 2.25 eV. We therefore conclude that the strong tail seen in $\alpha(\omega)$ when measured using optical transmission [Fig. 1(a)] cannot be accounted for by linear absorption. In order to enhance laser action that is usually limited by self-absorption, it is thus necessary to minimize this absorption tail, which otherwise increases the optical loss coefficient at the lasing wavelength.

Band II, peaking at 3.9 eV, is a matter of controversy. In substituted PPV derivatives it has been assigned either to charge conjugation symmetry breaking, or short PPV segments in the film.[10,11,22] In unsubstituted PPV, however no charge conjugation symmetry breaking due to substitution occurs. In contrast, we cannot rule out the possibility of having short chain segments in our films giving rise to the appearance of a small absorption band such as band II. Band III, peaking at 4.9 eV, is due to localized to delocalized and delocalized to localized transitions. Whereas band IV, peaking at 6 eV, originates from localized state transitions within the benzene molecular orbital states.[22] Miller *et al.* found in a stretched oriented poly(2-methoxy-5(2′ethyl-hexyloxy)-1-4-phenylene vinylene) sample that the absorption bands I, II, and IV is oriented parallel to the chain while the absorption band III is polarized off axis in the ratio 2:1 (perpendicular to parallel).[27]

In order to fit the asymmetric absorption spectrum of PPV for energies in band I, we have used the following model. First, we calculated the electron-vibration contribution to $\alpha(\omega)$ using the Huang–Rhys (HR) ansatz:

$$\alpha_{dd}(\omega)\propto \mathrm{Im}\left[e^{-S}\mu_{01}^2\sum_{p=0}^{\infty}\frac{S^p}{p!}\frac{1}{(\omega_{1B_u}-i\Gamma+p\nu-\omega)}\right], \quad (1)$$

where α_{dd} is the delocalized π-π^* absorption, ω_{1B_u} is the energy of the $1B_u$ exciton, Γ is the inhomogeneous broadening parameter and set to be 20 meV, S is the HR parameter, μ_{01} is the transition dipole moment, and ν is the phonon frequency. In the remainder we write the energy of the $1B_u$ exciton, $E(1B_u)$ as $E_{1B_u}=\omega_{1B_u}-i\Gamma$.

Second, since most films of PPV contain chains with a distribution of conjugation lengths (CL) due to mechanical distortion, *cis* bonds, defects, imperfections, impurities, and cross-links, we include in $\alpha(\omega)$ a CL distribution [see Fig. 1(b), inset], α_{CL}, by performing a weighted average over the shifted energy states around the mean $1B_u$ energy:[30]

$$\alpha_{CL}(\omega)\propto\int_{-\delta}^{+\delta}W(E')\alpha(E_{1B_u}+E';\omega)dE'. \quad (2)$$

The CL distribution in Eq. (2) is approximated by an asymmetric Gaussian weight function, $W(E)$, as follows:

$$W(E')=\frac{1.13}{B}\frac{\exp\{-[E'/B-F(u)]^2\}}{1+\exp\{-[E'/B-F(u)]\}}, \quad (3)$$

where

TABLE I. The best-fitting parameters for the two-component absorption fit (A1 and A2) of PPV. Here Δq is the relative displacement of the electronic states parabolas $E_A(q_A)$ and $E_B(q_B)$, where q is the configurational coordinate of the state, S is the Huang–Rhys parameter, and $h\nu$ is the phonon energy. The CL distribution width (γ) and asymmetry (δ) are used as free parameters, and they are numerically evaluated from the distribution. The relative strength of the bimodal chain-length distribution in the fits are given by I_A.

Parameter	A1	A2
$E(1B_u)$	2.589 eV	2.705 eV
Δq_1	1.65	2.40
$S=(\Delta q_1)^2/2$	1.36	2.88
$h\nu$	0.19 eV	0.19 eV
γ	0.16 eV	0.19 eV
δ	2.11	2.11
I_A	0.27	0.73

$$F(u)=\frac{0.95}{1+e^{u}}-0.475. \tag{4}$$

The parameters B and u in Eq. (4) allow the width and asymmetry of $W(E')$ to be varied without changing the position of the mean $1B_u$ energy.[30] From $W(E')$ we numerically evaluated the width $\gamma=a+b$ and the asymmetry $\delta=b/a$ of the CL distribution, where a and b are defined as the distance from the mean energy to the half-height points [see Fig. 1(b), inset].

In Fig. 1(a) we show the result of the calculated $\alpha(\omega)$ with the parameters given in Table I. In comparison with the data, obviously it is impossible to simultaneously fit the well-pronounced vibronic feature on the low-energy side *and* the broad absorption at high-energy side, when using only a single CL distribution function. For the CL distribution we therefore introduce in the calculation two CL components, $W_1(E)$ and $W_2(E)$ [shown as thin solid lines in Fig. 1(a)], having different mean energies and different line shapes (manifested by different HR factors). The two CL distributions have mean energy $E(1B_u)$ of 2.59 eV and 2.71 eV, respectively, where the higher-energy component has a relative strength of 2.7.

We can intuitively understand the two CL components as due to a bimodal CL distribution. In the more ordered parts of the film we have longer CL, and hence also lower $E(1B_u)$ with a smaller HR parameter. Whereas in the disordered part, the average CL is shorter and therefore $E(1B_u)$ is higher, with an increased Huang-Rhys parameter due to localization. A bimodal distribution with similar intensity ratios has been used by Mulazzi *et al.* to analyze both absorption and resonant Raman spectra in PPV.[45]

Another possible explanation of the two CL distribution functions may be the existence of *cis* bonds in the PPV film, which increase disorder by disrupting the CLS and interfere with the packing in the film. According to Son *et al.*,[46] we can estimate the amount of *cis* bonds in our converted PPV film from the intensity ratio of the infrared absorption band that are due to *cis* vibrations at 877.5 cm^{-1} to that of *trans* vibrations at 964.2 cm^{-1}. In Fig. 2 we show the ir spectrum of our PPV film, spun from methanol precursor solution on a KBr substrate that was measured using a Fourier transform ir

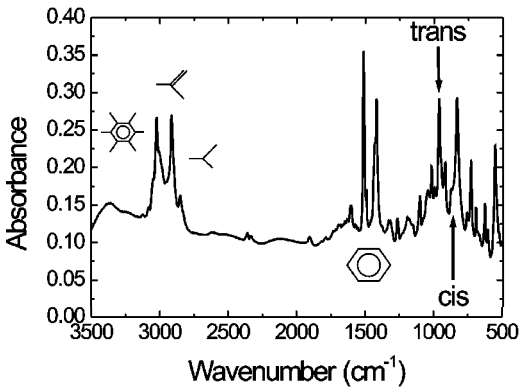

FIG. 2. ir-absorption spectrum in PPV showing that the ratio of *cis* (877.5 cm^{-1}) to *trans* (964.2 cm^{-1}) bonds is $<20\%$. The absorption lines around 3000 cm^{-1} are from various C-H stretching vibrations in different surroundings, as indicated in the figure. The two bands at 1515 cm^{-1} and 1421 cm^{-1} are from aromatic ring vibrations.

spectrometer. From the above-mentioned ir vibration intensity ratio we estimate the *cis*/*trans* ratio in our film to be about 20%. This may sufficiently disturb the CL distribution $W(E)$ in our film to form two CL components.

We note that even when we include two CL distribution functions we still cannot fit $\alpha(\omega)$ in the spectral region below band III. The dashed line in Fig. 1(a) is the difference spectrum between the calculated and measured $\alpha(\omega)$, revealing the existence of an additional absorption band at 3.9 eV, *which we attribute to absorption band II*. It is possible that this band is due to a weak charge-conjugation symmetry breaking, as previously discussed by Martin *et al.*,[33] or the presence of short segments as suggested by Chandross and Mazumdar.[11]

The room-temperature PL band and the PL QY action spectrum are shown in Fig. 3. The phonon replica in the PL band are well pronounced with five sidebands separated by the same spacing as in $\alpha(\omega)$, namely 190 meV. This energy may be related to the PPV C=C stretching mode vibration.[46] The PL QY spectrum $\eta_{PL}(E)$ shows a flat response with an onset at $E=2.5$ eV, as expected for high-quality PPV films.[47]

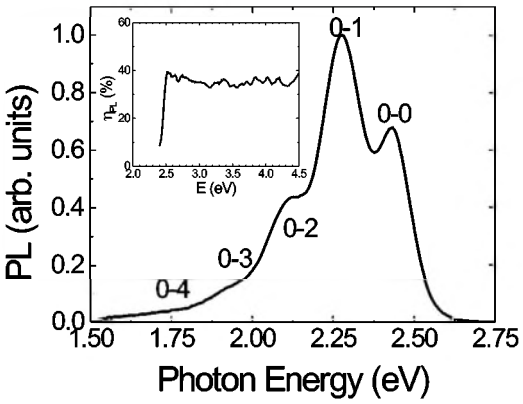

FIG. 3. The normalized room-temperature PL spectrum of PPV with assigned phonon sidebands. The inset shows the scaled PL action spectrum that consists of a step-function response with onset at about 2.5 eV. The absolute value of $\eta_{PL}=33\%$ at 3.55 eV excitation was measured with an integrating sphere.

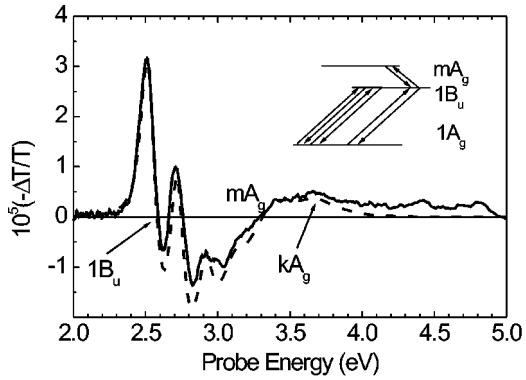

FIG. 4. The electroabsorption spectrum of PPV (full line). The dashed line is the best-fit calculation using the summation over states model that is schematically shown at the top of the figure.

TABLE II. The best fitting parameters for the EA spectrum of PPV. The parameters are the same as in Table I. The relative strength of the bimodal chain-length distribution in the fits is given by $I_{mA_g}(I_{kA_g})$.

Parameter	EA
$E(1B_u)$	2.589 eV
Δq_1	1.20
$S=(\Delta q_1)^2/2$	0.72
$h\nu$	0.19 eV
γ	0.13 eV
δ	2.77
$E(mA_g)$	3.40 eV
$E(kA_g)$	3.70 eV
$\Delta q_{2,3}$	−0.60
I_{mA_g}/I_{kA_g}	0.82

$\eta_{PL}(E)$ was normalized at 3.5 eV by the absolute PL QY, $\eta_{PL}=33\%$, which we measured with an integrating sphere.[48] A flat $\eta_{PL}(E)$ response means that the thermalized excitons have a certain probability of radiative recombination, independent of the excitation photon energy, E. The obtained flat $\eta_{PL}(E)$ response also validates our experimental capability to correctly measure $\eta(E)$ of photoexcitations. We note that $\eta_{PL}(E)$ is very different from the action spectra of triplets and polarons presented below in Sects. III E and III F, respectively.

B. Electroabsorption spectroscopy

Electroabsorption (EA) spectroscopy is a powerful optical method suitable for studying the excited electronic states in polymers and oligomers. In EA we use an ac electric field at frequency f to modify the electronic states in the material. Due to the quadratic Stark effect in polymers, we measure the changes $\Delta\alpha(\omega)$ in the absorption $\alpha(\omega)$ at $2f$. For the EA measurements we used an interlocking finger electrode geometry[30] with an interelectrode separation of 40 μm. The applied electric field was kept below 10^5 V/cm, and the EA signal was measured to be quadratic with the applied voltage.

The EA spectrum of PPV is shown in Fig. 4. There are three main EA spectral features in the range of absorption band I [Fig. 1(a)]. At low $\hbar\omega$ there is a derivativelike feature that crosses zero at 2.58 eV, followed by two well-pronounced phonon replicas at 2.77 eV and 2.96 eV, respectively. At higher energies there are two EA bands emerging at 3.40 eV and 3.70 eV, respectively, with no corresponding features in the absorption spectrum. We conjecture that these are due to strongly coupled even-parity states, mA_g and kA_g, respectively, with different relative strengths. The transitions $1A_g \rightarrow mA_g$ and $1A_g \rightarrow kA_g$ are symmetry forbidden, but the symmetry-breaking external electric field makes these transitions somewhat allowed by borrowing oscillator strength from the $1A_g \rightarrow 1B_u$ transition.[11] At higher energies the EA spectrum is always positive, which might suggest that there exist a sequence of even-parity states whose number is much larger than two.

The redshifted EA spectrum (see Fig. 4) cannot be explained in a pure two-level system. Any perturbation leads to a blueshifted EA spectrum caused by a further splitting of the two levels. The redshifted EA spectrum necessarily implies (i) the existence of a higher-lying third level with (ii) a stronger coupling to the second level than between levels one and two.[30] For fitting the EA spectrum we note that to a good approximation the EA spectrum is proportional to the imaginary part of the third-order optical susceptibility[30]

$$\left|-\frac{\Delta T}{T}\right| = \frac{4\pi\omega}{nc}\mathrm{Im}\chi^{(3)}(-\omega,\omega,0,0)F^2 d, \tag{5}$$

where n is the refractive index, c is the speed of light, and F is the strength of the applied electric field. To calculate the third-order optical susceptibility, $\chi^{(3)}$ we used the summation over states (SOS) model, originally proposed by Orr and Ward[49] and further developed for π-conjugated polymers by Liess *et al.*[30] For a centrosymmetric polymer such as PPV, we included three essential states, namely the $1A_g$, $1B_u$, and $mA_g(kA_g)$.

For the EA spectrum fit we included vibrational effects via the Franck–Condon approximation with harmonic potential and the CL distribution component for the longer chains taken from the fit of $\alpha(\omega)$ [see Eq. (2)]. For π-conjugated polymers it has been shown that the contribution to $\chi^{(3)}$ is strongly proportional to the conjugation length L, where $\chi^{(3)}\sim L^p$ with $p\gg 1$.[50] The short CL distribution that was used to fit $\alpha(\omega)$ at large $\hbar\omega$ is therefore not important for the EA calculation, and the long CL distribution dominates. The asymmetric Gaussian CL distribution [see Eq. (3)] used in the EA fit is shown in Fig. 4, inset. By including four essential states in the calculation, namely $1A_g$, $1B_u$m and two even-parity states mA_g and kA_g we could fit the EA spectrum as shown in Fig. 4 with parameters given in Table II. Martin *et al.*, have included the nB_u state in their EA calculations in PPV,[33] but found that the relative strength of the nB_u contribution is much smaller compared to the contribution of mA_g and kA_g states. From the obtained fit to the data we conjecture that only three essential excited states are sufficient to analyze the experimental EA spectrum.

When inspecting the EA spectrum obtained in our measurements, it is obvious the absence of Franz–Keldysh (FK) oscillations at the continuum band onset, as seen in polydiacetylene single crystals.[51] However, the higher-lying even-parity state, namely mA_g, may be considered to be the lower

limit of the continuum band, with the fine FK oscillations destroyed by the disorder in the film.[52] In this case, we can get an estimate of the $1B_u$ exciton binding energy E_b, using the relation

$$E_b \geqslant E(mA_g) - E(1B_u) \simeq 0.8 \text{ eV}, \tag{6}$$

in good agreement with Martin *et al.*[33] The binding energy estimated here is the energy difference between the fully relaxed $1B_u$ exciton and the fully relaxed nB_u exciton, which lies energetically just above the mA_g exciton, and can be considered as the onset of the continuum band. The lower limit of the binding energy here is considerably higher than estimates that originate from indirect electrical measurements, ranging from a few meV up to 0.4 eV.[19,53] However, the binding energy estimated from the indirect electrical measurements is defined as the energy difference between the creation of two fully separated and relaxed charge carriers of opposite sign, which is different from our definition here; care must therefore be exercised when comparing binding energies measured by different techniques.[54]

The theoretical models using negligible on-site electron interaction U cannot explain the large binding energy in the neutral manifold that we obtained here. It is therefore important to incorporate in any model calculations a relatively large electron–electron interaction to explain the observed optical properties in PPV, and also in other π-conjugated polymers. We further note that the binding energy measured here is not far off from the measured binding energies of 0.5 eV that is commonly accepted in polydiacetylenes.[52]

C. Photoinduced absorption spectroscopy

The PA spectrum of a PPV film spun on sapphire substrate and measured at 80 K is shown in Fig. 5(a). As previously reported,[2] the PA spectrum is composed of two main PA bands, where the higher-energy band can be decomposed into two independent bands [shown in Fig. 5(a)] based on their different frequency and temperature dependencies.[2,55] The two PA bands at 0.5 eV (P_1) and 1.9 eV (P_2) are correlated, whereas the band T_1 at 1.5 eV is not correlated with the other two bands. Also PADMR shows (see Sec. III D) that T_1 PA band is correlated with spin-1, whereas P_1 and P_2 PA bands are correlated with spin-1/2 excitations. We therefore identify P_1 and P_2 PA bands as the two allowed transitions of long-lived polaron excitations (charge $\pm e, S = 1/2$), whereas T_1 is a transition in the triplet manifold ($T \rightarrow T^*$), related to the long-lived triplet excitons (charge neutral, $S=1$). Recent model calculations show[11,15] that the most strongly coupled excited state to the $1\,^3B_u$ in the triplet manifold is the $m\,^3A_g$. We therefore identify T_1 at 1.5 eV with the transition $1\,^3B_u \rightarrow m\,^3A_g$ in the triplet manifold.

The intensity dependence [see Fig. 5(b)] of the in-phase signal, (measured with respect to the laser modulation) for both P_1 and T_1 shows a crossover from linear to almost $\sqrt{I}$ behavior; this is expected for bimolecular recombination kinetics. This type of recombination kinetics is clear for polarons since $P^+ + P^- \rightarrow$ ground state. Bimolecular recombination kinetics for triplets can only be explained by triplet–triplet annihilation ($dT_1/dt \sim -BT_1^2$, where B is the bimolecular recombination rate coefficient). Triplet–triplet annihilation is possible if the exciton diffusion is substantial. Partee *et al.*[56] have suggested from delayed fluorescence that triplet–triplet annihilation to form singlet excitons is important in substituted PPVs. Considering that the unsubstituted PPV forms a more close-packed structure than the substituted PPVs, we suggest that triplet diffusion could be even more important in unsubstituted PPV films. We note however, that Hertel *et al.*[57] found that in a ladder type polymer, the delayed fluorescence is due to recombination of electron–hole pairs, rather than triplet–triplet annihilation.

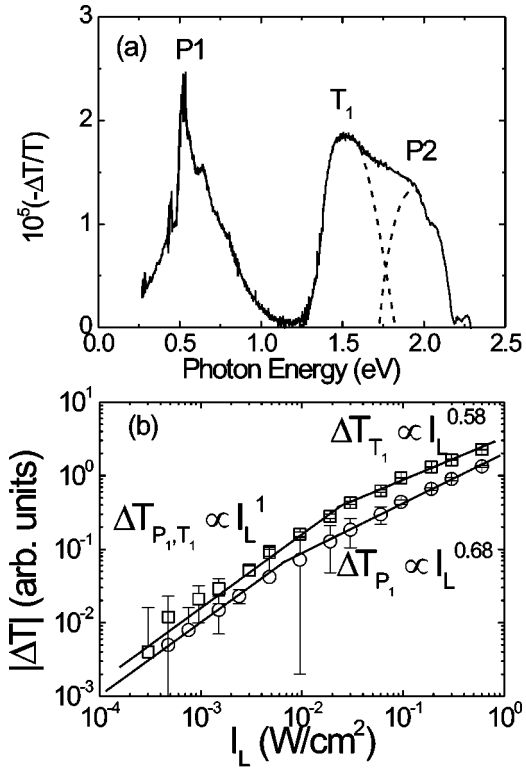

FIG. 5. (a) The photomodulation spectrum of PPV measured at 80 K. The PA bands P_1, P_2, and T_1 are assigned. (b) The intensity dependence of the P_1 (circles) and T_1 (squares) bands are shown, both showing bimolecular behavior at higher pump intensities.

D. Optically detected magnetic resonance spectroscopy

The H-PADMR spectrum of PPV measured at $\hbar\omega = 1.5eV$ is shown in Fig. 6(b). It contains two $\delta T > 0$ resonance bands; one at $H_0 = 1008$ G ($g \simeq 2, S = 1/2$ excitations) and the other at $H_1 \simeq 260$ G ($g \simeq 8$, half-field resonance of $S=1$ excitations). We note the extremely weak PA ($\Delta T/T \approx 10^{-5}$) and PADMR ($\delta T/T \approx 10^{-7}$) signals that are caused by the small density of traps, i.e., impurities, and defects in our PPV film; this is consistent with the high-PL QY that we measured in this film. The small PADMR signal has not allowed us to obtain continuous λ-PADMR spectra for the spin-1/2 and spin-1 excitations. However, to further separate between these two types of excitations we measured the H-PADMR spectrum at selected λ following the various PA bands in the PA spectrum (Fig. 6).

The wave-function extent of the lowest-lying triplet exciton may be obtained from the half-field triplet powder pat-

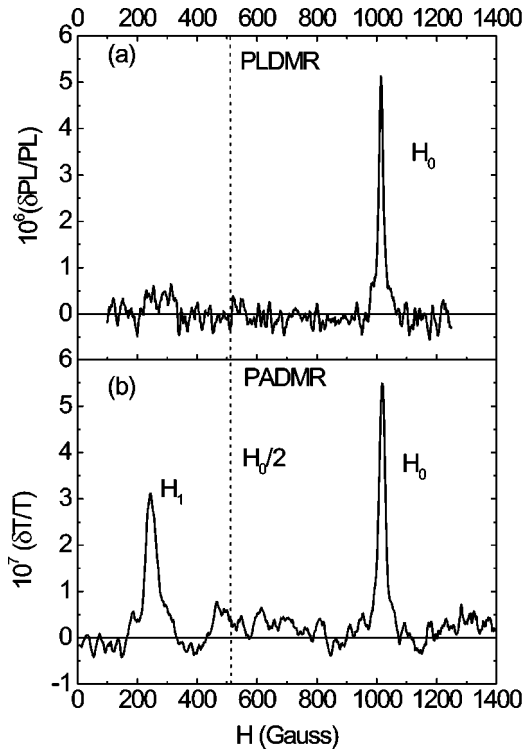

FIG. 6. (a) The *H*-PLDMR spectrum of PPV at 10 K, where only one resonance at H_0 ($S=1/2$) is seen. (b) The *H*-PADMR spectrum of PPV measured at $\hbar\omega=1.5$ eV. The two $\delta T>0$ resonances at H_0 ($S=1/2$) and at $H_1<H_0/2$ that is emphasized by the vertical dashed line ($S=1$, "half-field") are assigned.

tern at H_1. This resonance is shifted from $(1/2)H_0$ due to the zero-field splitting parameters, D and E in the Zeeman spin Hamiltonian:

$$\mathcal{H}=g\beta\ \bar{\mathbf{H}}\cdot\bar{\mathbf{S}}+D(s_z^2-1/3s^2)+E(s_x^2-s_y^2), \tag{7}$$

where $\bar{s}=\bar{s}_1+\bar{s}_2$, $\bar{s}_1$ and $\bar{s}_2$ are the spins 1/2 of the electron and hole, respectively, $g\beta\bar{\mathbf{H}}\cdot\bar{\mathbf{S}}$ is the magnetic Zeeman splitting term and the zero-field splitting (ZFS) parameters D and E are given by:

$$D=\frac{3g^2\beta}{4}\left\langle\Psi_T\left|\frac{r^2-3z^2}{r^5}\right|\Psi_T\right\rangle, \tag{8}$$

$$E=\frac{3g^2\beta}{4}\left\langle\Psi_T\left|\frac{y^2-x^2}{r^5}\right|\Psi_T\right\rangle. \tag{9}$$

In Eqs. (8) and (9), $\Psi_T(\bar{r})$ is the triplet wave function and $\bar{r}=\bar{r}_1-\bar{r}_2$, where $\bar{r}_1$ and $\bar{r}_2$ are the electron and hole vector coordinates, respectively. A useful approximation for the triplet wave-function extent, R, can be then derived[58]

$$R^3=2.78\times10^4/D, \tag{10}$$

where R is measured in Å and D is in G.

The half-field triplet powder pattern has a strong maximum at H_1 given by[58]

$$H_1=\frac{H_0}{2}\left[1-\left(\frac{D+E}{H_0}\right)^2\right]^{1/2}, \tag{11}$$

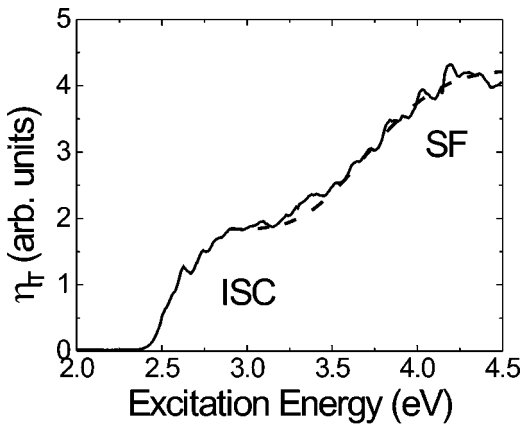

FIG. 7. The triplet QY action spectrum (full line) as deduced from the T_1 PA excitation spectrum. Two photogenerated processes, namely, intersystem crossing and singlet fission, are assigned. The dashed line is the best fit to the singlet fission model as described in the text.

where $H_1<H_0$. Using Eq. (11) and assuming an axial symmetric $\Psi_T(\bar{r})$, i.e., $E=0$ [Eq. (9)] we obtain from $H_1=260$ G and $D=(H_0^2-4H_1^2)^{1/2}$, a ZFS parameter $D=864$ G. Consequently from Eq. (10) we estimate the triplet wave function extent R in PPV to be $R=3.2$Å. This shows that the lowest-lying triplet in PPV (the 1^3B_u state) is highly localized and may be treated as a molecular Frenkel-type exciton. This is in contrast to the singlet $1B_u$ state, which has been shown to extend in PPV over about six repeat units.[4] The short triplet wave-function extent implies that the lowest-lying triplet energy in PPV lies deep inside the optical gap, consistent with a large singlet–triplet energy splitting.

E. Triplet exciton energy level

In a previous communication we have shown a way to obtain the triplet energy levels in PPV,[59] based on the action spectrum of the T-T^* PA band. The T_1 excitation spectrum is shown here in Fig. 7. One photogeneration process starts at the optical gap and has a flat energy response, similar to that of the PL QY spectrum. We identify this process as mainly due to thermalized excitons, consistent with intersystem crossing (ISC) from excitons at the bottom of the lowest-lying excitonic states.[60] The second operative triplet photogeneration process, with an onset at $E\simeq3.1$ eV, is due to unthermalized excitons. There are two possible processes that occur during the ultrafast exciton thermalization. These are upper excited-state transfer[61] and singlet fission (SF).[62] The maximum efficiency for upper excited-state transfer is at energies close to higher triplet states. The plateau at $\simeq4.4$ eV should then be the second lowest triplet state. In EA (see above in Sec. III B) we measured the mA_g state at 3.4 eV, 1 eV lower than the plateau. Hence, upper excited-state transfer cannot explain our data.

Singlet fission,[62,63] on the contrary, is a process where a singlet exciton (Ex) decomposes into a pair of triplets with opposite spins: $\mathrm{Ex}\rightarrow T_\uparrow+T_\downarrow$. The energy barrier for such a process is given by $E=2E_T$, where E_T is the triplet energy, $E_T\equiv E(1^3B_u)$. The prediction from theory is a single step function at $E=2E_T$.[62,63] However, the experimental $\eta_T(E)$ curve increases very slowly above the onset at $2E_T$. The

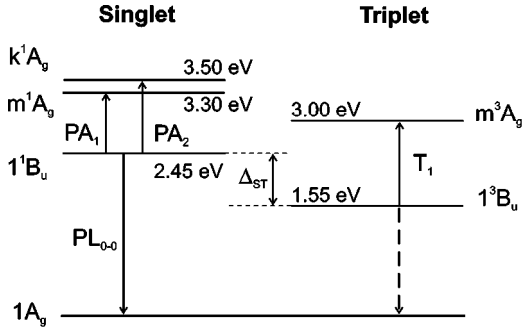

FIG. 8. The important excited energy levels of PPV in the neutral manifold. All energies we obtained from our cw spectroscopies here, except the bands PA_1 and PA_2 that were observed in the transient ps pump and probe spectroscopy (Ref. 60).

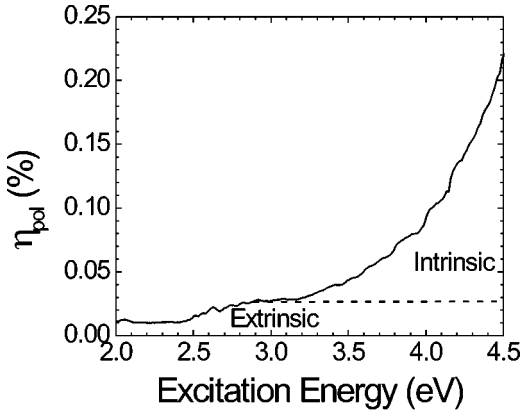

FIG. 9. The polaron PA (P1) QY action spectrum of PPV, normalized as described in the text. The separation between the extrinsic and intrinsic photogeneration processes is marked by the thin dashed line.

slow increase in the triplet QY spectrum towards high E may be explained by making the following two assumptions:[42] (i) E_T is spread out inhomogeneously due to the CL distribution and (ii) singlet fission may be accompanied, just like any other electronic transition, by emission of strongly coupled phonons. We obtained $E_T=1.55$ eV and $S_T=1.5$ from the experimental data using the singlet fission model.[64] We note that the triplet-exciton Huang–Rhys parameter is considerably larger than that for the singlet exciton obtained for the EA spectrum [where $S_{\mathrm{EA}}=(\Delta q_1)^2/2=0.72$], consistent with the more localized triplet-exciton wave function. For PPV, there is no direct measurement of $E(T)$ from phosphorescence, but pulse radiolysis experiments[65,66] on PPV derivatives have measured $E(T)$ at 1.3 to 1.5 eV, in good agreement with our measurements.

In Fig. 8, we summarize the energy levels and optical transitions in the neutral manifold obtained in this and previous work.[59] The excitonic absorption bands, PA_1 and PA_2, however, were observed in ps pump and probe spectroscopy,[60] since the exciton lifetime is on the order of 0.5 ns, much too fast to be observed in our cw measurements. Within the singles configuration interaction it was shown by Shimoi and Abe that the upper state in triplet absorption is degenerate with the $m\,^1A_g$.[8] Within a theory that went to higher order it was shown by Shimoi and Mazumdar that this upper state occurs actually below the $m\,^1A_g$, and hence this state, the $m\,^3A_g$, is an exciton, assuming that the $m\,^1A_g$ is an exciton.[68] We can then get a lower limit estimate of the singlet exciton binding energy $E_b(\min)$ in PPV: $E_b(\min)=T-\Delta_{\mathrm{ST}}=0.55$ eV. This value is in agreement with $E_b=0.8$ eV obtained from the EA spectroscopy summarized above.

The large $\Delta_{\mathrm{ST}}\simeq 0.9$ eV found here can be tied to the important role of the electron–electron interaction in these materials. Models with relatively large on-site electron–electron interaction[8–11,15,67] and recent *first principles* calculations[16] are all in agreement with our findings. We note that Gartstein *et al.* calculated $\Delta_{\mathrm{ST}}=0.6$ eV involving a small on-site Coulomb interaction U (within an exciton basis formalism).[22] But in models with negligible U, the T_1 transition should be of the order of Δ_{ST}. In our experiment we measured *both* Δ_{ST} and T_1 transitions, and found that they are not degenerate. Furthermore, the negligible U models cannot explain the large exciton binding energies in the neutral manifold that we obtained here. The necessity to involve large U in model calculations is important for further theoretical studies of the electronic states and related optical properties in π-conjugated polymers.

F. Polaron excitation spectrum

In Fig. 9 we show the polaron photogeneration quantum yield $\eta_p(E)$ measured at low light intensity I, where the polaron density is proportional to I [see Fig. 5(b)]. In the linear regime of the intensity dependence we can estimate the experimental QY at 3.65 eV, using the absorption cross section for polarons, $\sigma_p=2\times 10^{-15}$ cm^{-2} measured by Harrison *et al.*[69] For this estimate we use the equation

$$N_{SS}=(-\Delta T/T)/\sigma_p d=gI\eta\tau, \tag{12}$$

where $\tau^{-1}\simeq 500\ \mathrm{s}^{-1}$ is obtained from the polaron PA frequency response.[55] Since $d\sim 200$ nm, we can estimate the experimental QY from Eq. (12) to be about 0.5% at 3.55 eV (with an uncertainty of 0.5%).

Similarly as for $\eta_T(E)$ spectrum, the $\eta_p(E)$ spectrum also contains two processes: a step function response at $E=2.5$ eV, followed by a monotonically increasing function of E, with an onset at approximately 3.3 eV, i.e., at the threshold for the generation of free charge carriers, $E_{th}=E_{1B_u}+E_b$. A similar E dependence was previously measured in the action spectra of photocurrent[70–73] and light-induced electron spin resonance.[74–76] This shows that the charge carriers are photogenerated through an intrinsic process, and not via a photoemission process as suggested in Ref. 70.

Since the thermalization process is much shorter than the exciton lifetime in PPV, we expect that the process of exciton dissociation ($\mathrm{Ex}\rightarrow P^-+P^+$) at impurities to be dominated by thermalized excitons. The action spectrum (at low intensities) of this "extrinsic" process will then have a step-function response at the optical gap, similar to $\eta_{\mathrm{PL}}(E)$ in Fig. 3, inset. At higher excitation densities (10^{15} cm^{-2}) the polaron generation has been shown by Kraabel *et al.*, to be quadratic in exciton density or probably due to an exciton–exciton annihilation process.[77] The second process, which must then be due to *hot* excitons, is intrinsic in nature. Above

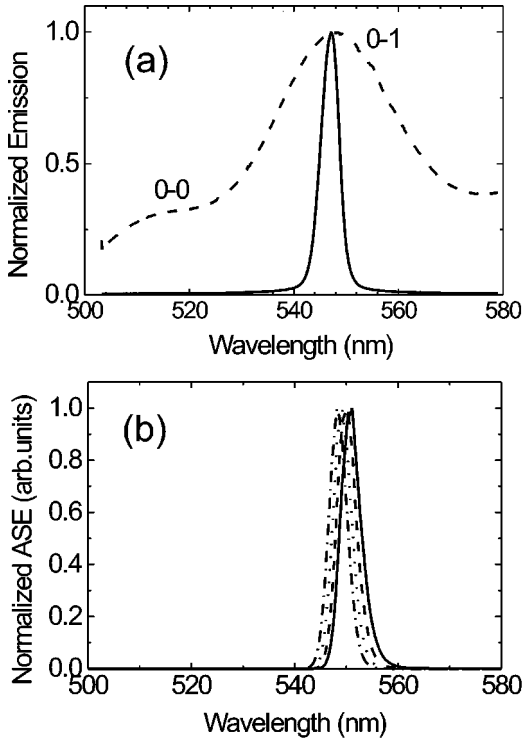

FIG. 10. (a) The normalized PL emission spectrum of a PPV thin film. The dashed line corresponds to a pump fluence of 4.3μJ/cm^2 (43.0 kW/cm^2) and the full line is for a pump fluence of 143 μJ/cm^2 (1.43 MW/cm^2) that shows spectral narrowing or ASE. (b) The calculated ASE spectrum using Eq. (13) (normalized for clarity). Note the blueshift in emission that occurs upon reduction of the self-absorption. Different values of relative bleaching were used: 0% (full line), 25% (dashed line), 50% (dotted line), and 75% (dash-dotted line).

3.3 eV free-electron–hole pairs with zero total momentum are formed. According to the Onsager model by increasing the photon energy the *e-h* pair gains more excess energy, which leads to a more efficient initial *e-h* separation. The electron–hole pairs thermalize down by phonon emission and scattering processes and form either excitons (both singlets and triplets at various rates[78]) or free polarons, if their separation distance after thermalization is larger than the Coulomb radius, $r_C = e^2/4\pi\varepsilon\varepsilon_0 kT$.[79] Disorder plays an important role in the process, since we do not observe any Franz–Keldysh oscillations signatures of a real continuum band in PPV. However, the mA_g state at 3.3 eV may be taken as the onset of the continuum band, in excellent agreement with the polaron excitation spectrum.

G. Laser action in thin PPV films and microcavities

1. Amplified spontaneous emission

The first report on spectral narrowing (SN) in π-conjugated polymers was by Moses, who reported stimulated emission and lasing from a methoxy derivative of PPV in solution.[80] Yan *et al.*, reported pump–probe-type stimulated gain in both stretched-oriented films and solution.[37,38] Another major breakthrough was reported in 1996 when three groups independently reported laser action in π-conjugated polymer thin films.[81–83]

We have observed SN in PPV films as shown in Fig. 10(a). When pumping above a threshold fluence, I_0 of 20 $\mu J/cm^2$, which corresponds to an exciton density $N_0 = 1.8 \times 10^{18}$ cm^{-3} and a power density of 200 kW/cm^2, then the broad PL spectrum (FWHM$\simeq$100 nm) collapses into a narrow line (FWHM=4.5 nm) at the 0-1 transition that occurs at around 547 nm (2.26 eV). The emission also slightly blueshifts upon spectral narrowing. The PL 0-1 band has its maximum at 548 nm, whereas the narrow band has its emission maximum at 546 nm. I_0 is the same as that reported earlier for laser action in PPV films by the Denton *et al.*[84] and in poly(2,5-dioctyloxy-*p*-phenylene vinylene) DOO PPV by Froler *et al.*[85] The mechanism for SN has been interpreted as amplified spontaneous emission (ASE) aided by waveguiding in the film.[84]

The ASE intensity can be written for a high gain medium as

$$I(L) \approx \left(\frac{\pi h c^2 \Omega}{\lambda^5}\right) \Delta\lambda\, e^{g_{\text{eff}} L}, \tag{13}$$

where the effective gain coefficient $g_{\text{eff}} > 0$. In Eq. (13) c is the speed of light, Ω is the appropriate solid angle of the excitation geometry, and $\Delta\lambda$ is the width of the emission band. When we take absorption loss into account, then g_{eff} can be estimated from the relation

$$g_{\text{eff}} = \sigma N - \alpha, \tag{14}$$

where σ is the exciton optical cross section at the laser frequency, N is the exciton density, and α is the absorption coefficient. The effective gain spectrum is reminiscent of the PL spectrum with the subtraction of the absorption coefficient. By assuming a spectral shape for σ based on the room-temperature PL spectrum, we calculated the effective gain spectra in PPV, using the absorption coefficient obtained from the PDS spectrum [see Sec. III A and Fig. 1(b)]. The effective optical gain cross section, σ_g may be calculated from σ using the relation[86,87]

$$\sigma_g(\lambda) = \left(\frac{\lambda}{\lambda_0}\right)^4 \sigma(\lambda_0), \tag{15}$$

where we assume $\sigma(\lambda_0) = 4 \times 10^{-16}$ cm^2 at the peak of the 0-1 PL band at $\lambda_0 = 547$ nm.[36] Based on σ_g in Eq. (15) we can estimate from Eq. (14) the exciton threshold density for ASE (positive effective gain) to be $N_0 \simeq 1.5 \times 10^{18}$ cm^{-3}, in excellent agreement with the experimental threshold value. The effective gain spectrum does, however, suggest that ASE would first occur at the 0-2 transition rather than the 0-1 (or 0-0) transition (see Fig. 11). Denton *et al.* studied the ps PA in unsubstituted PPV and found that photobleaching was observed only for the 0-1 transition;[40] the 0-2 transition being too deep in the gap. We therefore suggest that the photobleaching is not homogeneous throughout the absorption spectrum, but is more pronounced at the 0-1 transition. Since the spectral diffusion is very fast, on the order of a few picoseconds,[88] we expect that the relaxed, thermalized excitons end up on longer chain segments. Chain segments with higher energies do not have substantial absorption in the visible range and the photobleaching is therefore more pronounced in the red part of the main absorption band.

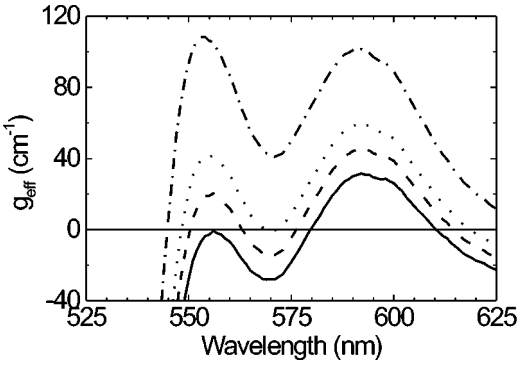

FIG. 11. The effective gain spectrum $g_{\text{eff}}(\lambda)$ of a PPV film calculated from the PL spectrum and PDS absorption spectrum. For $g=\sigma N$ we used $\sigma N=150$ cm^{-1} (full line), $\sigma N=160$ cm^{-1} (dashed line), $\sigma N=170$ cm^{-1} (dotted line), and $\sigma N=200$ cm^{-1} (dash-dotted line).

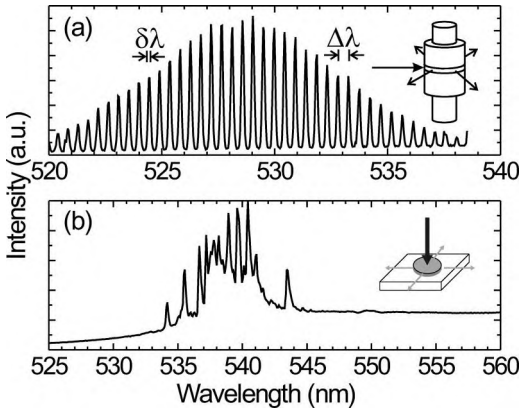

FIG. 12. (a) Laser emission spectrum of a PPV microring of 125 μm in diameter; the intermode spacing is $\Delta\lambda=0.45$ nm and the spectral width is $\delta\lambda=1$ Å. (b) Lasing from a microdisk of 128 μm in diameter. The pump excitation and collection geometries for the two cases are shown in the respective insets.

In Fig. 10(b) we show the calculated ASE spectrum, using Eqs. (13)–(15), and a PL spectrum that consists of a single Lorentzian with the same width and position as that of the PL 0-1 band. By decreasing the absorption coefficient in Eq. (14) due to the photobleaching discussed above, we qualitatively obtained the blueshift of the maximum ASE as observed experimentally [Fig. 10(b)]. We note that π-conjugated polymers are a class of materials with high phonon energies ($\sim$190 meV), which makes ASE switching between different phonon sidebands possible.[89]

2. PPV microlasers

We have also fabricated PPV microlasers. In Fig. 12 we show lasing from (a) a microring of 125 μm diameter and (b) a microdisk with diameter of 128 μm. The spectral width of the microring laser modes is limited in resolution by our spectrometer to about 1 Å. This may be used to estimate the microcavity Q value, $Q=\lambda/\Delta\lambda\gtrsim 5000$, which is probably limited by self-absorption.[85] The dominant mode in the microring lasers is the waveguide mode,[85] of which the intermode spacing is given by

$$\Delta\lambda=\frac{\lambda^2}{\pi D n_{\text{eff}}}, \tag{16}$$

where D is the diameter of the microring and n_{eff} is the mode effective refractive index. The experimentally observed intermode spacing ($\Delta\lambda=0.45$ nm) can be fitted using this relation with $n_{\text{eff}}=1.58$ [see Fig. 12(a)]. The reason for the low mode effective refractive index that we obtained here compared to the polymer $n=1.7$ is the proximity of the PPV film to the fiber core with $n=1.46$, coupled with the mode distribution inside the film. In the microdisks, on the other hand, no clear laser modes could be obtained, probably due to multimode operation.

IV. CONCLUSIONS

We used a multitude of optical cw spectroscopies to study the long-lived neutral and charged photoexcitations in PPV thin films, as well as laser action in both thin films and microcavities. We found that the linear absorption at the main π-π^* transition ($\simeq$3 eV) cannot be completely explained by involving a single CL distribution; a bimodal CL distribution better explains the shape of absorption band I. The low-energy tail of the optical absorption was shown to extend far in the ir region, as measured by photothermal deflection spectroscopy. However, the much higher absorption tail that is usually measured by optical transmission is due to scattering in the PPV microcrystals.

From the EA spectrum we obtained the $1B_u$ exciton at $E(1B_u)=2.59$ eV and the higher-lying even-parity excitons $E(mA_g)=3.4$ eV and $E(kA_g)=3.7$ eV. From these energies we estimated the exciton binding energy in PPV, $E_b(\text{min})=E(mA_g)-E(1B_u)=0.8$ eV. We used PA and PADMR spectroscopies to estimate the extent of the triplet-exciton wave function. We found that the triplet is localized on one benzene unit of the PPV chain. The quantum efficiency spectrum for the triplet-exciton photogeneration consists of two contributions; the intersystem crossing and, at higher energies, singlet fission. From the onset of the singlet fission process at $E_{\text{SF}}=2E_T$, we could estimate the energy of the lowest-lying triplet exciton, $1\,^3B_u$, at 1.55 eV. The singlet–triplet splitting Δ_{ST} is therefore about 0.9 eV, showing the existence of a large electron–electron interaction in PPV.

From the polaron PA action spectrum we identified two photogeneration processes in PPV: an extrinsic process having a step-function spectral response at 2.4 eV and an intrinsic process that is due to generation of free charge carriers having an onset at about 3.3 eV. From the intrinsic carrier photogeneration process we estimate the long-lived polaron generation efficiency to be 0.5% at 365 nm.

We also observed laser action in thin PPV films and microcavities such as microrings and microdisks. The effective gain spectrum of PPV was calculated and the estimated threshold exciton density for laser action was found to be in good agreement with the experimentally measured threshold value of 2×10^{18} cm^{-3}. Lasing from microrings shows several narrow waveguide modes with an intermode spacing of 0.45 nm that corresponds to a mode effective refractive index $n_{\text{eff}}=1.45$. The spectral width of the laser modes is resolution limited and gives an estimate of the laser quality factor

Q. For the microring cavity we found $Q>5000$, which is limited by self-absorption in the polymer film.

ACKNOWLEDGMENTS

The authors acknowledge M. Delong for help with the synthesis and the ir spectra, J. Viner for help with the PDS spectrum, and fruitful discussions with S. Mazumdar and P. Lane. This work was partially supported by DOE Grant No. FG-03-96 ER 45490 and NSF, Grant No. DMR-02-02790. One of us (R.Ö.) acknowledges funding from The Swedish Academy of Engineering Sciences in Finland, the Neste Ltd. Foundation, and the Academy of Finland Project No. 48853.

[1] J. H. Burroughes, D. D. C. Bradley, A. R. Brown, R. N. Marks, K. Mackay, R. H. Friend, P. L. Burn, and A. B. Holmes, Nature (London) **347**, 539 (1990).
[2] N. F. Colaneri, D. D. C. Bradley, R. H. Friend, P. L. Burn, A. B. Holmes, and C. W. Spangler, Phys. Rev. B **42**, 11670 (1990).
[3] C. J. Baker, O. M. Gelsen, and D. D. C. Bradley, Chem. Phys. Lett., **201**, 127 (1993).
[4] K. Pichler, D. A. Halliday, D. D. C. Bradley, P. L. Burn, R. H. Friend, and A. B. Holmes, J. Phys. C **5**, 7155 (1993).
[5] J. M. Leng, S. Jeglinski, X. Wei, R. E. Benner, Z. V. Vardeny, F. Guo, and S. Mazumdar, Phys. Rev. Lett. **72**, 156 (1994).
[6] G. da Costa and E. W. Conwell, Phys. Rev. B **48**, 1993 (1993).
[7] M. J. Rice and Y. N. Gartstein, Phys. Rev. Lett. **73**, 2504 (1994).
[8] Y. Shimoi and S. Abe, Phys. Rev. B **49**, 14 113 (1994).
[9] M. Chandross, S. Mazumdar, S. Jeglinski, X. Wei, Z. V. Vardeny, E. W. Kwock, and T. M. Miller, Phys. Rev. B **50**, 14702 (1994).
[10] Y. Shimoi and S. Abe, Synth. Met. **78**, 219 (1996).
[11] M. Chandross and S. Mazumdar, Phys. Rev. B **55**, 1497 (1997).
[12] W. Barford, R. J. Bursill, and M. Yu. Lavrentiev, J. Phys.: Condens. Matter **10**, 6429 (1998).
[13] S. Brazovskii, N. Kirova and A. R. Bishop, Opt. Mater. **9**, 465 (1998).
[14] S. Brazovskii, N. Kirova, A. R. Bishop, V. Klimov, D. McBranch, N. N. Barashkov, and J. P. Ferraris, Opt. Mater. **9**, 472 (1998).
[15] M. Yu. Lavrentiev, W. Barford, S. J. Martin, H. Daly, and R. J. Bursill, Phys. Rev. B **59**, 9987 (1999).
[16] M. Rohlfing and S. G. Louie, Phys. Rev. Lett. **82**, 1959 (1999).
[17] A. Ruini, M. J. Caldas, G. Bussi, and E. Molinari, Phys. Rev. Lett. **88**, 206403 (2002).
[18] *Primary Photoexcitations in Conjugated Polymers; Molecular Excitons vs. Semiconductor Band Model*, edited N. S. Sariciftci (World Scientific, Singapore, 1998).
[19] J. L. Bredas, J. Cornil, and A. J. Heeger, Adv. Mater. **8**, 447 (1996).
[20] S. N. Dixit, D. Guo, and S. Mazumdar, Phys. Rev. B **43**, 6781 (1991).
[21] S. Mazumdar and F. Guo, J. Chem. Phys. **100**, 1665 (1994).
[22] Y. N. Gartstein, M. J. Rice, and E. M. Conwell, Phys. Rev. B **52**, 1683 (1995).
[23] M. Chandross, S. Mazumdar, M. Liess, P. A. Lane, Z. V. Vardeny, M. Hamaguchi, and K. Yoshino, Phys. Rev. B **55**, 1486 (1997).
[24] D. Beljonne, J. Cornil, D. A. dos Santos, and J. L. Bredas, J. Chem. Phys. **111**, 2829 (1999).
[25] T. W. Hagler, K. Pakbaz, K. F. Voss, and A. J. Heeger, Phys. Rev. B **44**, 8652 (1991).
[26] T. W. Hagler, K. Pakbaz, and A. J. Heeger, Phys. Rev. B **49**, 10968 (1994).
[27] E. K. Miller, D. Yoshida, C. Y. Yang, and A. J. Heeger, Phys. Rev. B **59**, 4661 (1999).
[28] U. Lemmer, R. Fischer, J. Feldman, R. F. Mart, J. Yang, A. Greiner, H. Bässler, E. O. Göbel, H. Heesel, and H. Kurz, Chem. Phys. Lett. **203**, 28 (1993).
[29] S. V. Frolov, Z. Bao, M. Wohlgenannt, and Z. V. Vardeny, Phys. Rev. B **65**, 205209 (2002).
[30] M. Liess, S. Jeglinski, Z. V. Vardeny, M. Ozaki, K. Yoshino, Y. Ding, and T. Barton, Phys. Rev. B **56**, 15712 (1997).
[31] Y. Shimoi and S. Abe, Synth. Met. **91**, 363 (1997).
[32] S. J. Martin, H. Mellor, D. D. C. Bradley, and P. L. Burn, Opt. Mater. **9**, 88 (1998).
[33] S. J. Martin, D. D. C. Bradley, P. A. Lane, H. Mellor, and P. L. Burn, Phys. Rev. B **59**, 15133 (1999).
[34] R. H. Friend, R. W. Gymer, A. B. Holmes *et al.*, Nature (London) **397**, 121 (1999).
[35] U. Rauscher, H. Bässler, D. D. C. Bradley, and M. Hennecke, Phys. Rev. B **42**, 9830 (1990).
[36] M. Yan, L. J. Rothberg, F. Papadimitrakopoulus, M. E. Galvin, and T. M. Miller, Phys. Rev. Lett. **72**, 1104 (1994).
[37] M. Yan, L. J. Rothberg, B. R. Hsieh, and R. R. Alfano, Phys. Rev. B **49**, 9419 (1994).
[38] M. Yan, L. J. Rothberg, E. W. Kwock, and T. M. Miller, Phys. Rev. Lett. **75**, 1992 (1995).
[39] I. D. W. Samuel, G. Rumbles, and C. J. Collinson, Phys. Rev. B **52**, 11573 (1995).
[40] G. J. Denton, N. Tessler, N. T. Harrison, and R. H. Friend, Phys. Rev. Lett. **78**, 733 (1997).
[41] V. I. Klimov, D. W. McBranch, N. Barashkov, and J. Ferraris, Phys. Rev. B **58**, 7654 (1998).
[42] M. Wohlgenannt, W. Graupner, G. Leising, and Z. V. Vardeny, Phys. Rev. Lett. **82**, 3344 (1999).
[43] D. Chinn, M. Delong, A. Fujii, S. Frolov, K. Yoshino, and Z. V. Vardeny, Synth. Met. **102**, 930 (1999).
[44] R. A. Wessling and W. J. Settineri, U.S. Patent No. 3,480,525 (1969).
[45] E. Mulazzi, A. Ripamonti, J. Wery, B. Dulieu, and S. Lefrant, Phys. Rev. B **60**, 16519 (1999).
[46] S. Son, A. Dodabalapur, A. J. Lovinger, and M. E. Galvin, Science **269**, 376 (1995).
[47] N. T. Harrison, G. R. Hayes, R. T. Phillips, and R. H. Friend, Phys. Rev. Lett. **77**, 1881 (1996).
[48] N. C. Greenham, I. D. W. Samuel, G. R. Hayes, R. T. Phillips, Y. A. R. R. Kessener, S. C. Moratti, A. B. Holmes, and R. H. Friend, Chem. Phys. Lett., **241**, 89 (1995).
[49] B. J. Orr and J. F. Ward, Mol. Phys. **20**, 513 (1971).
[50] Z. Shuai and J. L. Brédas, Phys. Rev. B **44**, 5962 (1991).
[51] L. Sebastian and G. Weiser, Phys. Rev. Lett. **46**, 1156 (1981).
[52] A. Horvath, G. Weiser, C. Lapersonne-Meyer, M. Schott, and S. Spagnoli, Synth. Met. **84**, 553 (1997).
[53] S. F. Alvarado, P. F. Seidler, D. G. Lidzey, and D. D. C. Bradley, Phys. Rev. Lett. **81**, 1082 (1998).
[54] E. M. Conwell and H. A. Mizes, Synth. Met. **78**, 210 (1996).
[55] R. Österbacka, M. Shkunov, D. Chinn, M. Wohlgenannt, M. Delong, J. Viner, and Z. V. Vardeny, Synth. Met. **101**, 226 (1999).
[56] J. Partee, E. L. Frankevich, B. Uhlhorn, J. Shinar, Y. Ding, and T. J. Barton, Phys. Rev. Lett. **82**, 3673 (1999).
[57] D. Hertel, Yu. V. Romanovskii, B. Schweitzer, U. Scherf, and H. Bässler, Synth. Met. **116**, 139 (2001).
[58] Z. V. Vardeny and X. Wei, In *Handbook of Conducting Polymers*, 2nd ed., edited by T. A. Skotheim and R. L. Elsenbaumer (Dekker, New York, 1988), p. 639.
[59] R. Österbacka, D. Chinn, M. Wohlgenannt, and Z. V. Vardeny, Phys. Rev. B **60**, 11253 (1999).
[60] S. V. Frolov, M. Liess, P. A. Lane, W. Gellermann, Z. V. Vardeny, M. Ozaki, and K. Yoshino, Phys. Rev. Lett. **78**, 4285 (1997).
[61] M. Pope and C. E. Svenberg, *Electronic Processes in Organic Crystals (Clarendon, Oxford, 1982)*.
[62] R. H. Austin, G. L. Baker, S. Etemad, and R. Thompson, J. Chem. Phys. **90**, 6642 (1989).
[63] B. Kraabel, D. Hulin, C. Aslangul, C. Lapersonne-Meyer, and M. Schott, J. Chem. Phys. **227**, 83 (1998).
[64] M. Wohlgenannt, W. Graupner, R. Österbacka, G. Leising, D. Comoretto, and Z. V. Vardeny, Synth. Met. **101**, 267 (1999).
[65] A. Monkman, H. D. Burrows, M. da G. Miguel, I. Hamblett, and S. Navaratnam, Chem. Phys. Lett. **307**, 303 (1999).
[66] A. P. Monkman, H. D. Burrows, L. J. Hartwell, L. E. Horsburgh, I. Hamblett, and S. Navaratnam, Phys. Rev. Lett. **86**, 1358 (2001).
[67] A. Shukla, Phys. Rev. B **65**, 125204 (2002).
[68] Y. Shimoi and S. Mazumdar, Synth. Met. **85**, 1027 (1997).
[69] M. G. Harrison, K. E. Ziemelis, R. H. Friend, P. L. Burn, and A. B. Holmes, Synth. Met. **55**, 218 (1993).
[70] D. Moses, C. Soci, P. Miranda, and A. J. Heeger, Chem. Phys. Lett., **350**, 531 (2001).
[71] X. Wei, S. A. Jeglinski, and Z. V. Vardeny, Synth. Met. **85**, 1215 (1997).
[72] A. Köhler, D. A. dos Santos, D. Beljonne, Z. Shuai, J.-L. Brédas, A. B. Holmes, A. Kraus, K. Müllen, and R. H. Friend, Nature (London) **392**, 903 (1998).

[73] S. Barth, H. Bässler, H. Rost, and H. H. Hörhold, Phys. Rev. B **56**, 3844 (1997).
[74] K. Murata, S. Kuroda, Y. Shimoi, S. Abe, T. Noguchi, and T. Ohnishi, Synth. Met. **91**, 359 (1997).
[75] K. Murata, Y. Shimoi, S. Abe, S. Kuroda, T. Noguchi, and T. Ohnishi, Chem. Phys. Lett. **227**, 191 (1998).
[76] S. Kuroda, K. Marumoto, H. Ito, N. C. Greenham, R. H. Friend, Y. Shimoi, and S. Abe, Chem. Phys. Lett. **325**, 183 (2000).
[77] B. Kraabel, V. I. Klimov, R. Kohlman, S. Xu, H.-L. Wang, and D. W. McBranch, Phys. Rev. B **61**, 8501 (2000).
[78] M. Wohlgenannt, X. M. Jiang, Z. V. Vardeny, and R. A. J. Janssen, Phys. Rev. Lett. **88**, 197401 (2002).
[79] D. M. Pai and R. Enck, Phys. Rev. B **11**, 5163 (1975).
[80] D. Moses, Appl. Phys. Lett. **60**, 3215 (1992).
[81] N. Tessler, G. J. Denton, and R. H. Friend, Nature (London) **382**, 695 (1996).
[82] F. Hide, M. A. Diaz-Garcia, B. J. Schwartz, M. R. Andersson, Q. Pei, and A. J. Heeger, Science **273**, 1833 (1996).
[83] S. V. Frolov, M. Ozaki, W. Gellerman, Z. V. Vardeny, and K. Yoshino, Jpn. J. Appl. Phys. **35**, L1138 (1996).
[84] G. J. Denton, N. Tessler, M. A. Setevens, and R. H. Friend, Adv. Mater. **9**, 547 (1997).
[85] S. Frolov, M. Shkunov, Z. V. Vardeny, and K. Yoshino, Phys. Rev. B **56**, R4363 (1997).
[86] C. W. Lee, K. S. Wong, J. D. Huang, S. V. Frolov, and Z. V. Vardeny, Chem. Phys. Lett. **314**, 564 (1999).
[87] J. D. Huang, S. V. Frolov, Z. V. Vardeny, C. W. Lee, and K. S. Wong, Synth. Met. **116**, 61 (2001).
[88] G. R. Hayes, I. D. W. Samuel, and R. T. Phillips, Phys. Rev. B **52**, 11569 (1998).
[89] M. Shkunov, R. Österbacka, A. Fujii, K. Yoshino, and Z. V. Vardeny, Appl. Phys. Lett. **74**, 1648 (1999).